ROLE OF KINETIC EXCHANGE AND COULOMB INTERACTION IN BONDING OF HYDROGEN MOLECULAR SYSTEMS AND EXCITED STATES*

Maciej Hendzel

Institute of Applied Computer Science, Jagiellonian University
Łojasiewicza 11, 30-348 Kraków, Poland

Piotr Kuterba, Józef Spałek†

Department of Condensed Matter Theory and Nanophysics
Institute of Theoretical Physics, Jagiellonian University
Łojasiewicza 11, 30-348 Kraków, Poland

Received 30 April 2026, accepted 4 May 2026,
published online 15 May 2026

We present a detailed investigation of the electronic structure and bonding characteristics of hydrogen-based molecular systems (H_2^+, H_2, H_2^-) using the Exact Diagonalization Ab Initio (EDABI) approach within the framework of combined first and second quantization. By analyzing the relative contributions of kinetic exchange and effective Coulomb interactions, we provide a comprehensive understanding of covalency, atomicity, and ionicity as a function of interatomic distances. Our approach leverages exact solutions of the extended Heitler–London model to quantify these interactions, extending the analysis to the discussion of properties of excited states and the dissociation limit of these molecules. The findings reveal significant differences in bonding characteristics, particularly highlighting the stability and bonding nature of the neutral H_2 molecule compared to its ionic counterparts. This study not only enhances our understanding of molecular interactions in hydrogen systems but also demonstrates the potential of the EDABI approach in developing more accurate computational models in quantum chemistry.

DOI:10.5506/APhysPolB.57.5-A18

1. Introduction

Fundamental understanding of molecular electronic structure and bonding is crucial for various applications in chemistry and physics. Despite the

* Presented at the Concepts in Strongly Correlated Quantum Matter Conference (CSCQM), Kraków, Poland, 20–22 November, 2025.

† Corresponding author: jozef.spalek@uj.edu.pl

publication of numerous remarkable works, the discussion on selected aspects of chemical bonding remains intense, even for relatively simple systems like diatomic molecules [1]. In our view, this ongoing debate is related to the advancement of numerical methods, which remain interpretative challenges despite achieving highly accurate numerical results with the appropriate level of complexity and sophistication.

To provide a brief outline of this discussion, it is worth mentioning works related to the ambiguity of the concepts of ionicity and covalency in chemical bonds [2, 3], as well as attempts to explain the covalency of the bond in the hydrogen molecule and other diatomic molecules [1, 4–6]. We have contributed to this discussion by providing the complementary characteristics of the chemical bond such as the atomicity and true covalency [7, 8] or our recent work about entanglement correlations as the alternative bonding characteristic [9].

In this paper, we use the Exact Diagonalization Ab Initio (EDABI) approach to investigate the detailed electronic structure of hydrogen-based molecular systems, specifically H_2^+, H_2, and H_2^-. We employ the formalism of second quantization to express the Hamiltonian and wavefunctions, enabling a clear and concise representation of the electronic states. The Hamiltonian we consider includes all two-electron interactions in the Fock space that appear in the two-orbital model of the Heitler–London-type. The whole analysis is based on the exact solution of the extended Heitler–London model of the H_2 molecule and its concomitant optimization with respect to the molecular orbital size.

One of the key aspects we explore is the concept of the bonding characteristics, namely covalency, atomicity, and ionicity, within the context of molecular dissociation. By examining the bonding factors as a function of interatomic distance, we provide an insight into the nature of chemical bonding and the evolution between different physical regimes. The analysis is based on the already mentioned exact solutions of the extended Heitler–London model, allowing us to rigorously quantify the contributions of kinetic exchange interactions and effective Coulomb interactions to the total bonding. Furthermore, we extend our investigation to the excited states of hydrogen molecules and discuss how they compare to the ground state.

2. Method

The total electronic energy of a system is expressed as the sum of the kinetic and interaction energy parts. The kinetic energy term in Hartree–Fock corresponds to the average kinetic energy of non-interacting electrons in the effective potential generated by the other electrons. On the other hand, the exchange kinetic energy refers to the contribution to the total

kinetic energy that arises from the exchange interaction between identical particles, such as electrons. This is a quantum mechanical effect resulting from the indistinguishability of identical particles.

To single out those exchanges and other contributions, we start from two general forms of the Hamiltonian in the Fock space

$$\hat{\mathcal{H}} = \sum_{ij\sigma} t_{ij} \hat{a}^\dagger_{i\sigma}\, \hat{a}_{j\sigma} + \frac{1}{2} \sum_{\substack{ijkl \\ \sigma\sigma'}} V_{ijkl}\, \hat{a}^\dagger_{i\sigma}\, \hat{a}^\dagger_{j\sigma'}\, \hat{a}_{l\sigma'}\, \hat{a}_{k\sigma}\,, \tag{1}$$

where

$$t_{ij\sigma} \equiv \langle \phi_{i\sigma} | \mathcal{H}_1 | \phi_{j\sigma} \rangle\,, \tag{2}$$

and

$$V_{ijkl} = \langle \phi_{i\sigma} \phi_{j\sigma'} | V | \phi_{k\sigma'} \phi_{l\sigma} \rangle\,. \tag{3}$$

In these expressions, $t_{ij\sigma}$ represents the one-electron integrals, including kinetic energy and attraction of electrons by protons, while V_{ijkl} are the two-electron matrix elements, representing electron–electron Coulomb repulsion. The operators $\hat{a}^\dagger_{i\sigma}$ and $\hat{a}_{j\sigma}$ are the creation and annihilation operators for electrons in orbitals i and j with spin σ.

The general N-particle state $|\Phi_N\rangle$ in Fock space can be related to the corresponding N-particle wavefunction $\Psi_\alpha(\boldsymbol{r}_1, \ldots, \boldsymbol{r}_N)$ in Hilbert space as follows [10]:

$$\begin{aligned} |\Phi_N\rangle \;=\; & \frac{1}{\sqrt{N!}} \int \mathrm{d}^3\boldsymbol{r}_1 \ldots \mathrm{d}^3\boldsymbol{r}_N\, \Psi_N(\boldsymbol{r}_1, \ldots, \boldsymbol{r}_N) \\ & \times \hat{\Psi}^\dagger_{\sigma_1}(\boldsymbol{r}_1) \ldots \hat{\Psi}^\dagger_{\sigma_N}(\boldsymbol{r}_N)\, |0\rangle\,, \end{aligned} \tag{4}$$

where the field operator $\hat{\Psi}(\boldsymbol{r})$ is here approximated using a finite number M of wavefunctions $\{w_i(\boldsymbol{r})\}$

$$\hat{\Psi}(\boldsymbol{r}) \simeq \sum_{i=1}^{M} w_i(\boldsymbol{r}) \hat{a}_i\,, \tag{5}$$

composed of the Wannier–Mulliken function taken in the following form of molecular orbitals:

$$w_i(\boldsymbol{r}) = \beta(\psi_i(\boldsymbol{r}) - \gamma \psi_{i+1}(\boldsymbol{r}))\,. \tag{6}$$

Such functions are normalized and orthogonal, which leads to the following expressions for β and γ:

$$\beta \;=\; \frac{1}{\sqrt{2}} \sqrt{\frac{1 + \sqrt{1 - S^2}}{1 - S^2}}\,, \tag{7}$$

$$\gamma \;=\; \frac{S}{1 + \sqrt{1 - S^2}}\,, \tag{8}$$

where $S = \langle \psi_1(\boldsymbol{r}) | \psi_2(\boldsymbol{r}) \rangle$ denotes the overlap integral.

The approximate N-particle wavefunction can be then obtained by the reverse relation

$$\Psi_\alpha(\boldsymbol{r}_1,\ldots,\boldsymbol{r}_N)=\frac{1}{\sqrt{N!}}\sum_{i_1,\ldots,i_N=1}^{M}\langle 0|\hat{a}_{i_N}\ldots\hat{a}_{i_1}|\Phi_N\rangle w_{i_1}(\boldsymbol{r}_1)\ldots w_{i_N}(\boldsymbol{r}_N)\,. \quad (9)$$

In most general terms, the N-particle state can be expressed as follows:

$$|\Phi_N\rangle=\frac{1}{\sqrt{N!}}\sum_{j_1,\ldots,j_N=1}^{M}C_{j_1\ldots j_N}\hat{a}^\dagger_{j_1}\ldots\hat{a}^\dagger_{j_N}|0\rangle\,. \quad (10)$$

Substituting this into the N-particle wavefunction gives

$$\Psi_\alpha(\boldsymbol{r}_1,\ldots,\boldsymbol{r}_N)=\frac{1}{\sqrt{N!}}\sum_{i_1,\ldots,i_N=1}^{M}C_{i_1\ldots i_N}(A,S)w_{i_1}(\boldsymbol{r}_1)\ldots w_{i_N}(\boldsymbol{r}_N)\,, \quad (11)$$

where $C_{i_1\ldots i_N}(A,S)$ are the coefficients determined by the diagonalization. This also represents the Configurational Interaction (CI) wavefunction for N particles distributed among M states, with A and S indicating antisymmetrization (Slater determinant) for fermions or symmetrization for bosons, respectively. In CI, the wavefunction is expressed as a linear combination of Slater determinants, and the coefficients $C_{i_1\ldots i_N}(A,S)$ are optimized variationally.

The EDABI procedure involves diagonalization of the Hamiltonian matrix to find the exact wave function within a given basis set. The CI approach shares this feature but focuses on a finite basis set of M states, neglecting highly excited states to simplify the problem. In EDABI, excited states are determined on the same footing as the ground state.

The full electronic Hamiltonian for the two-orbital model was derived and discussed earlier [7, 8, 11]. In addition to that, we present schematically all physical processes which are involved in this Hamiltonian in Fig. 1. In the figure, ϵ_a denotes a single-particle energy of the electron in an atomic state and it is shown as an isolated electron with spin. The second microscopic parameter, hopping amplitude t, represents electron hopping between two neighboring atoms. It is represented schematically in Fig. 1 as an electron (green arrow) moving from one site to another. The U term accounts for the Coulomb repulsion between electrons on the same site. It is indicated in the figure by the purple arrow representing the repulsion between two electrons at the same site (green arrows indicate opposing spins). The K term represents the Coulomb interaction between electrons on different sites. The figure illustrates this as a repulsive force between electrons on adjacent

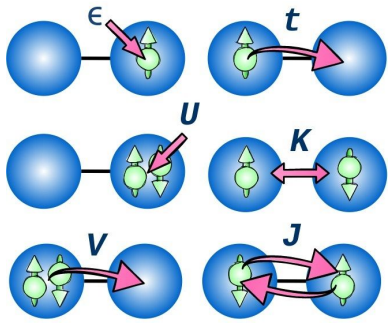

Fig. 1. Schematic illustration of various interaction processes within molecular systems, highlighting several key elements: single-particle excitation, electron hopping between adjacent sites, on-site Coulomb repulsion between electrons, direct exchange interaction between sites, inter-site Coulomb interaction, and indirect exchange interaction (superexchange). The green arrows represent particles with spin, while the pink arrows depict the pathways of these interactions.

sites (straight purple double arrow between two green arrows). The exchange integral J is shown in the figure as green arrows forming loops between two atoms occupied by two electrons with opposite spins suggesting the interaction involving an exchange of spin orientation. V is the so-called correlated hopping marked as the purple arrow from one atom to its neighbor indicating the hopping of an electron pair.

3. Results

Below, we discuss results for hydrogen-based molecular systems such as H_2^+, H_2, and H_2^- as functions of interatomic distance. This analysis will be helpful in specifying the molecular bonding and the role of the atomicity in it.

3.1. Hydrogen molecule excited states

We begin by analyzing the spin-excited states of the hydrogen molecule. In this context, spin-excited states comprise both the states with total spin $S = 1$ and $S = 0$. Our previous works [7, 8, 12] demonstrated that diagonalizing the Hamiltonian in second quantization form results in six states: three singlets and three triplets. We investigate these states, utilizing our bonding concepts of true covalency, atomicity, and ionicity [12, 13]. In Fig. 2, we present those bonding factors *versus* interatomic distance R for all six states, with eigenenergy expressions indicated on these plots.

In the bottom-left panel, we display those characteristics for the singlet ground state. The covalent contribution dominates at $R = R_{\text{eq}}$. There is a

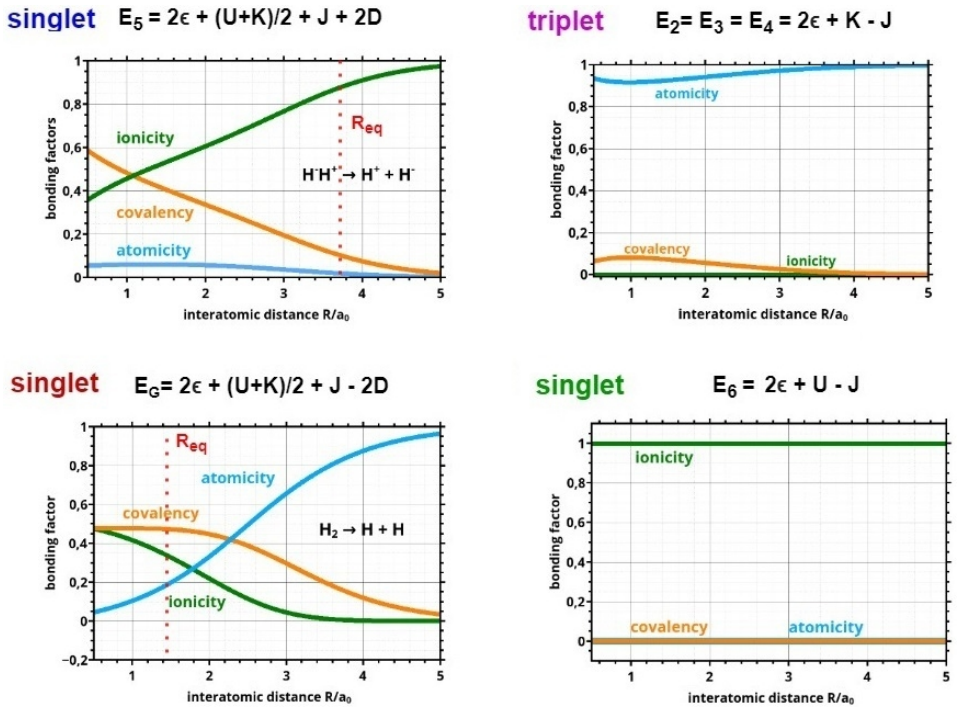

Fig. 2. The atomicity, ionicity, and true covalency for ground and excited states of the hydrogen molecule (H_2) as functions of interatomic distance R. The energy expressions for these states include contributions from kinetic energy, Coulomb interaction, and exchange terms. The bottom-left figure characteristics are those of the ground state.

small admixture of atomic contribution in that case. The ionic contribution is more noticeable than the atomic one, but as R increases, both those characteristics vanish, whereas the atomic part persists and reaches a maximal value in the $R \to \infty$ limit. The proper exact eigenvector in the coherent two-particle state can be written in the following form:

$$|\Psi_{\rm G}\rangle = C\left(\hat{a}^{\dagger}_{1\uparrow}\hat{a}^{\dagger}_{2\downarrow} - \hat{a}^{\dagger}_{1\downarrow}\hat{a}^{\dagger}_{2\uparrow}\right)|0\rangle - I\left(\hat{a}^{\dagger}_{1\uparrow}\hat{a}^{\dagger}_{1\downarrow} + \hat{a}^{\dagger}_{2\uparrow}\hat{a}^{\dagger}_{2\downarrow}\right)|0\rangle\ , \tag{12}$$

where C and I denote the covalent and ionic factors, respectively, with $C \equiv 4(t+V)/\sqrt{2D(D-U+K)}$, $I \equiv (D-U+K)/\sqrt{2D(D-U+K)} = \sqrt{(D-U+K)/2D}$, and $D \equiv \sqrt{(U-K)^2+16(t+V)^2}$. The evolution from covalent-dominated bonding ($C \gg A$) to the atomic limit $A \to 1, I \to 0$ is consistent with the intuitive picture resulting from the interpretation of

the behavior of the binding energy curve $E(R)$, where in the $R \to \infty$ limit, the molecule separates into two individual atoms. A is here the atomicity analyzed in detail earlier. This was the reason for introducing the atomicity, so the *true covalency* is defined by $\tilde{C} \equiv (C^2 - A^2)^{\frac{1}{2}}$ [7]. This expression for the τ is taken in the subsequent numerical analysis.

The top-left panel represents one of the spin-singlet states. In this case, ionicity contribution is dominant. The contribution of ionicity in this case is significantly smaller than that in the ground state, which is obvious due to the nature of the wave function. As the interatomic distance increases, covalency and atomicity approach zero, while ionicity reaches a value of unity.

The corresponding excited state can be expressed in the form

$$\begin{aligned} |5\rangle \;=\; & C\left(\hat{a}^{\dagger}_{1\uparrow}\hat{a}^{\dagger}_{2\downarrow} - \hat{a}^{\dagger}_{1\downarrow}\hat{a}^{\dagger}_{2\uparrow}\right)|0\rangle \\ & + I\left(\hat{a}^{\dagger}_{1\uparrow}\hat{a}^{\dagger}_{1\downarrow} + \hat{a}^{\dagger}_{2\uparrow}\hat{a}^{\dagger}_{2\downarrow}\right)|0\rangle \;. \end{aligned} \tag{13}$$

In this case, there are new functions C and I that represent covalent and ionic factor, where $C = 4(t+V)/\sqrt{2D(D+U-K)}$ and $I = \sqrt{(D+U-K)/2D}$. As shown in Fig. 2, this state has a small minimum at $R = 3.5a_0$. The molecule excited to this state has a metastable state of ionic character and, in the limit of infinite R, separates into atoms, but unlike for the ground state, it results in H^+ and H^- ions rather than two neutral atoms.

The top-right panel also depicts the excited triplet states. In this state, atomicity is shown to be the dominant characteristic for all interatomic distances. Covalency and ionicity remain minimal. Three degenerated triplet eigenvectors are of the form

$$\begin{cases} |1\rangle = \hat{a}^{\dagger}_{1\uparrow}\hat{a}^{\dagger}_{2\uparrow}|0\rangle\,, \\ |2\rangle = \hat{a}^{\dagger}_{1\uparrow}\hat{a}^{\dagger}_{2\downarrow}|0\rangle\,, \\ |3\rangle = \dfrac{1}{\sqrt{2}}\left(\hat{a}^{\dagger}_{1\uparrow}\hat{a}^{\dagger}_{2\downarrow} + \hat{a}^{\dagger}_{1\downarrow}\hat{a}^{\dagger}_{2\uparrow}\right)|0\rangle\,. \end{cases} \tag{14}$$

In this case, covalency, ionicity, and atomicity for the states with $S^z = \pm 1$ vanish, whereas for $S^z = 0$ states, it depends only on single-particle mixing parameters, β and γ. The top-right figure reflects this latter situation.

3.2. Bonding as a competition of dynamic processes

It is a well known, as demonstrated by Ruedenberg in his seminal work [14], that covalent bonding in the hydrogen molecule occurs as a result of the decrease in kinetic energy with the simultaneous increase in potential

energy. Regardless of the successes achieved in explaining the mechanisms of chemical bonding [14], the problem of ambiguity in results persists, as in the case of the LiH molecule, where the Molecular Orbital theory (MO) gives results different from the Valence Bond theory (VB). This issue was discussed by Pendas *et al.* [2] and also partly in our studies [7]. Furthermore, methods based on energy decomposition are not without flaws, as they heavily depend on the numerical methods they are based on, as was discussed in [15]. In this subsection, we propose an analysis of chemical bonding based on methods used in condensed matter physics, taking the hydrogen molecule as an example.

We start with the exact two-particle wave function, which was previously obtained by solving the extended Heitler–London model of the hydrogen molecule [7]. The wave function is of the form [8, 11, 12]

$$\begin{aligned}\Psi_0(\boldsymbol{r}_1,\boldsymbol{r}_2) &= \frac{2(t+V)}{\sqrt{2D(D-U+K)}}\Psi_{\rm cov}(\boldsymbol{r}_1,\boldsymbol{r}_2)\\ &\quad -\frac{1}{2}\sqrt{\frac{D-U+K}{2D}}\Psi_{\rm ion}(\boldsymbol{r}_1,\boldsymbol{r}_2)\\ &\equiv C\psi_{\rm cov}(\boldsymbol{r}_1,\boldsymbol{r}_2)-I\psi_{\rm ion}(\boldsymbol{r}_1,\boldsymbol{r}_2)\,. \end{aligned} \tag{15}$$

In the given expression, the wave function is represented as a linear combination of two terms: $\psi_{\rm cov}(\boldsymbol{r}_1,\boldsymbol{r}_2)$ and $\psi_{\rm ion}(\boldsymbol{r}_1,\boldsymbol{r}_2)$, and with the covalent C and ionic I factors being functions of microscopic parameters introduced in the previous subsection.

We consider next the physical picture of why the chemical homopolar bond is covalent when the kinetic exchange interaction complements the picture. To do that, we examine coefficients of the wave function from Eq. (15). The expression $D = \sqrt{16(t+V)^2+(U-K)^2}$ determines the energy denominator in the coefficients C and I of the wave function. The ratio of kinetic energy to potential energy can be written in the form

$$\begin{aligned} D &= (U-K)\sqrt{1+\left(\frac{4(t+V)}{U-K}\right)^2}\\ &= (U-K)\sqrt{1+\left(\frac{J_{\rm kex}}{U-K}\right)} =\\ &= E_{\rm eff}\sqrt{1+\left(\frac{J_{\rm kex}}{E_{\rm eff}}\right)}\,, \end{aligned} \tag{16}$$

where D, now the denominator, is expressed via the kinetic exchange integral $J_{\rm kex}\equiv 4(t+V)^2/(U-K)$ and effective Coulomb interaction $E_{\rm eff}\equiv U-K$.

In the quasiatomic regime, the $t + V$ contribution is much smaller than $U - K$, whereas in the covalent regime, it is predominant. But, as one can expect, the quasiatomic regime is far from $R = R_{\mathrm{eq}}$. In the $R \simeq R_{\mathrm{eq}}$ regime, $|t + V|$ contribution is of larger magnitude than $(U - K)$. Although, in general, the mechanism of covalent bond formation is consistent with that proposed by Ruedenberg, there are differences between his and our solution. In Ruedenberg's analysis, kinetic energy is the energy associated with the hopping of electrons, whereas the kinetic exchange interaction energy is related to the virtually resonating electrons in agreement with the notion of covalency. The potential energy in Ruendenberg's analysis is calculated based on the electrostatic interactions between charged particles (nuclei and electrons), whereas in our case, it is the difference between intraatomic and interatomic Coulomb repulsion, which is more natural in the discussion of ionic bonding.

In Fig. 3, the evolution of the two bonding factors, covalency and ionicity, is drawn as a function of the square root of the kinetic exchange to potential energy ratio. In our case, covalency dominates for all values of the ratio. What is new in our approach is that instead of decomposing the total energy into kinetic and potential components, we introduce effective parameters J_{kex} and E_{eff} based on the exact solution of the extended Heitler–London model. Note also that ionicity is absent when the virtual hopping is absent, pointing to the principal role of the correlation in a full description of the bond.

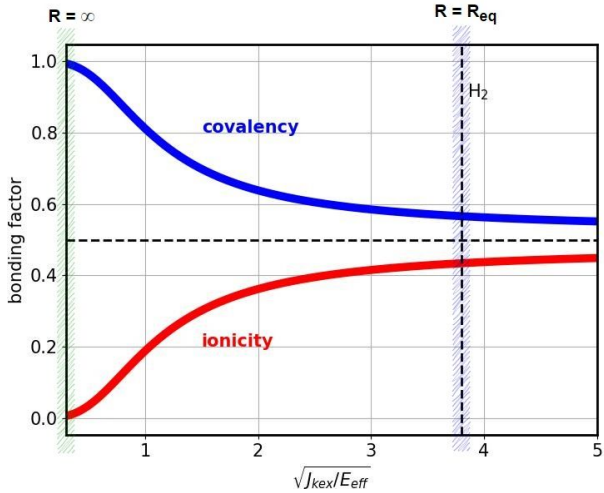

Fig. 3. Evolution of the bonding factors: bare covalency (without atomicity extracted) and ionicity for the H_2 molecule *versus* the square root of kinetic exchange and effective potential energy ratio. Two characteristic points are marked: the blue area is for that when $R = R_{\mathrm{eq}}$, the green area when $J_{\mathrm{kex}} \to 0$.

3.3. From one- to three-electron chemical bonding

We turn next to the hydrogen molecular cation H_2^+, with only one electron. We can write the second quantized wave functions in that case in the form

$$\left|\psi_+^{H_2^+}\right\rangle = \frac{1}{\sqrt{2}}\left(\hat{a}_1^\dagger + \hat{a}_2^\dagger\right)|0\rangle\,, \tag{17}$$

$$\left|\psi_-^{H_2^+}\right\rangle = \frac{1}{\sqrt{2}}\left(\hat{a}_1^\dagger - \hat{a}_2^\dagger\right)|0\rangle\,, \tag{18}$$

where only the bonding and antibonding single-particle orbitals appear, respectively. In this case, one can use the relation from Eq. (9) to calculate the corresponding Wannier functions of the form

$$\psi_+^{H_2^+}(\boldsymbol{r}) = \frac{1}{\sqrt{2(1+S)}}(w_1(\boldsymbol{r}) + w_2(\boldsymbol{r}))\,, \tag{19}$$

$$\psi_-^{H_2^+}(\boldsymbol{r}) = \frac{1}{\sqrt{2(1+S)}}(w_1(\boldsymbol{r}) - w_2(\boldsymbol{r}))\,, \tag{20}$$

which are transformed into the bonding molecular wave function to the atomic-based form

$$\begin{aligned}\psi_-^{H_2^+}(\boldsymbol{r}) = {} & \frac{\beta}{\sqrt{2(1+S)}}((\phi_1(\boldsymbol{r}) - \phi_2(\boldsymbol{r})) \\ & +\gamma(\phi_2(\boldsymbol{r}) - \phi_1(\boldsymbol{r}))\,,\end{aligned} \tag{21}$$

where ϕ_1 and ϕ_2 are the Slater wave functions centered on protons 1 and 2, respectively.

In the case of H_2^- ion, four states should be considered, leading to the construction of a 4×4 Hamiltonian, which yields two doubly degenerate states. For the lower energy state, the wave function in the language of second quantization takes the form

$$\left|\psi_G^{H_2^-}\right\rangle = \frac{1}{\sqrt{2}}\left(\hat{a}_{1\uparrow}^\dagger \hat{a}_{2\uparrow}^\dagger \hat{a}_{2\downarrow}^\dagger + \hat{a}_{1\downarrow}^\dagger \hat{a}_{2\uparrow}^\dagger \hat{a}_{2\downarrow}^\dagger\right)|0\rangle\,. \tag{22}$$

Equivalently, this form has the following form in terms of the Wannier functions

$$\begin{aligned}\psi_G^{H_2^-}(\boldsymbol{r}_1, \boldsymbol{r}_2, \boldsymbol{r}_3) = {} & \frac{1}{\sqrt{2}}(w_{1\uparrow}(\boldsymbol{r}_1) w_{2\uparrow}(\boldsymbol{r}_2) w_{2\downarrow}(\boldsymbol{r}_3) \\ & +w_{1\downarrow}(\boldsymbol{r}_1) w_{1\uparrow}(\boldsymbol{r}_2) w_{1\uparrow}(\boldsymbol{r}_3))\,.\end{aligned} \tag{23}$$

It can be transformed to the three-electron wave function consisting of linear combination of atomic functions

$$\begin{aligned}\psi_{\mathrm{G}}^{\mathrm{H}_2^-}(\boldsymbol{r}_1,\boldsymbol{r}_2,\boldsymbol{r}_3) \;=\; & \frac{\beta^3}{\sqrt{2}}(\phi_{1\uparrow}(\boldsymbol{r}_1)\phi_{2\uparrow}(\boldsymbol{r}_2)\phi_{2\downarrow}(\boldsymbol{r}_3)\\ & +\phi_{1\downarrow}(\boldsymbol{r}_1)\phi_{2\uparrow}(\boldsymbol{r}_2)\phi_{2\uparrow}(\boldsymbol{r}_3)\\ & +\phi_{1\uparrow}(\boldsymbol{r}_1)\phi_{1\downarrow}(\boldsymbol{r}_2)\phi_{2\uparrow}(\boldsymbol{r}_3)\\ & +\phi_{1\uparrow}(\boldsymbol{r}_1)\phi_{1\downarrow}(\boldsymbol{r}_2)\phi_{2\downarrow}(\boldsymbol{r}_3))\,. \end{aligned} \tag{24}$$

We elaborate now on those four states H_2^+ and H_2^-. The wave functions for H_2^+ consist of covalent bonding, where the single electron is spread over both nuclei, resulting in an intermediate bond strength. The bonding character is determined by both the overlap integral and mixing parameters (β, γ), whereas in the case of H_2, it is a more complex function of microscopic (t, U, V, K), as well as the mixing parameters.

The wave function of H_2 represents a stronger covalent bond case with an admixture of the ionic part, absent in the single electron of H_2^+.

The three-electron wave function of H_2^- (Eq. (24)) reveals a more involved picture, in which the differentiation between covalency and ionicity is not straightforward. It has a mixed resonant covalent-ionic bond character for which two electrons always occupy one atom and the third is resonating between the sites. Such a process results in a more complex picture, in which the overall bond energy is reduced as shown in Table 1.

Table 1. Comparison of bond lengths, E_{bond}, and $\frac{J}{E_{\mathrm{kex}}}$ (on one particle) for H_2^+, H_2, and H_2^-.

Molecule	R_{eq} (a_0)	E_{bond} [eV]	$\frac{J_{\mathrm{kex}}}{E_{\mathrm{eff}}}$
H_2^+	2.53	−1.7721	N/A
H_2	1.43	−4.0749	3.86
H_2^-	3.56	−2.1792	0.22

The presented values of the bond energy indicate that in either H_2^+ and H_2^- ions are lower than in the case of H_2, whereas the value of the ratio of effective kinetic exchange energy to potential energy is significantly larger than 1 only for H_2. Interestingly, the ratio for H_2^- takes a value significantly lower than 1.

In Fig. 4, the kinetic-exchange energy and the effective Coulomb interaction, both as a function of interatomic distance R, are compared for H_2 and H_2^-. From the bonding perspective, the plots provide an insight into

the nature of bonding in those molecules. The H_2 molecule exhibits characteristics typical of covalent bonding, with the kinetic exchange interaction comparable to the effective Coulomb interaction near the equilibrium distance (it is almost 4 times stronger). The effective kinetic energy decreases as the distance increases, still remaining larger than the effective potential energy. For H_2^-, the exchange interaction energy decreases steadily with the increasing R with the $J_{\rm kex}/E_{\rm eff}$ ratio less than 1 around $R_{\rm eq}$.

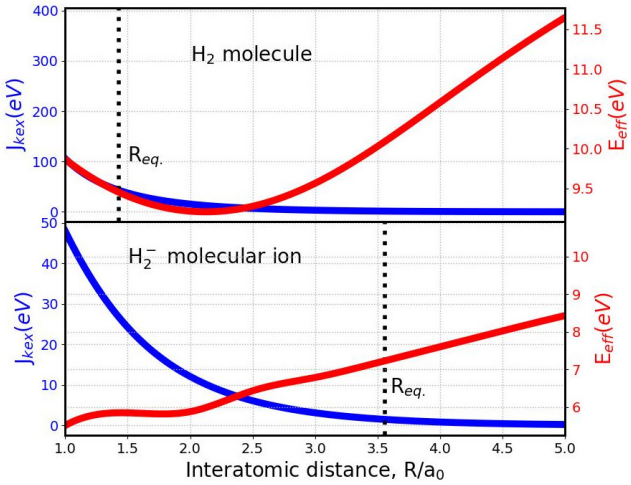

Fig. 4. Comparison of kinetic-exchange energy (left y-axis) and effective Coulomb interaction (right y-axis), both as a function of interatomic distance for the H_2 molecule (top) and H_2^- (bottom). The red curve in the bottom figure is not smooth, likely caused by numerical artifacts introduced during the calculations.

In Table 2, the basic quantities for H_2 and H_2^- are listed and compared at $R_{\rm eq}$. For H_2, the ground-state energy per particle is lower by about 3 eV as compared to that for H_2^-.

A smaller orbital size in the case of H_2 suggests that the electrons on orbitals are more tightly bound than in the H_2^- case. For the molecular ion, two α_0 values are provided, since the sizes of the $1s$ orbitals are not the same as they are occupied by either one or two electrons. The hopping parameters for these two systems indicate that electron mobility is significantly higher for H_2 (about four times larger). Additionally, Coulomb's repulsion magnitude is stronger in the case of H_2. Both interatomic and intraatomic values of repulsion are approximately twice as high as for the former. Similarly, the correlated hopping and exchange integrals are stronger in the neutral molecule.

Table 2. Comparison of key parameters: orbital size, ground-state energy per one particle, and microscopic parameters at the points of minimal energy for H_2 and H_2^-, respectively. α_0 is the inverse atomic orbital size at $R_{\rm eq}$ (the two values in H_2^- case correspond to the localized (tighter-bond) and resonating electron, respectively).

Parameter	H_2	H_2^-
$E_{\rm G}/N$ [eV]	−15.599	−12.87
α_0	0.839	1.25/1.33
t [eV]	−9.905	−1.487
U [eV]	22.490	13.99
K [eV]	13.007	6.705
V [eV]	−0.1578	−0.1265
J [eV]	0.2857	0.1238
$\frac{4(t+V)^2}{(U-K)}$ [eV]	37.39	1.604

Finally, the ratio $\frac{4(t-V)^2}{U-K}$ is 37.39 eV for H_2 and 1.604 eV for H_2^-, indicating a significantly stronger kinetic exchange interaction in the neutral molecule. This stronger kinetic exchange interaction enhances effective electron sharing (virtual hopping between the sites), promoting a much stronger covalent bonding in H_2.

4. Conlcusions

We have analyzed here the covalency, atomicity, and ionicity as the fundamental bonding characteristics for hydrogen-based systems, H_2, and H_2^-. The results provide a nuanced view of how bonds evolve between the different regimes: covalent, atomic, and ionic as the atoms move closer or separate from each other. In this work, we tested and developed the conceptual framework that employs the formalism of combined first and second quantization. We have discussed the exact solution of the extended Heitler–London model for the systems which allowed us to single out different contributions coming from kinetic energy, kinetic exchange, and effective Coulomb interactions. The analysis concentrates on the chemical bonding resulting from competition between those energies. By examining these interactions *versus* interatomic distance R, we offer an intuitive understanding of bonding nature, and in particular, highlight the evolution from covalent to ionic or atomic character in the ground and excited states, at least for the H_2 case.

This work was supported by grants No. UMO–2021/41/B/ST3/04070 and No. 2023/49/B/ST3/03545 from the National Science Centre (NCN), Poland.

REFERENCES

[1] Á. Martín Pendás, E. Francisco, «The role of references and the elusive nature of the chemical bond», *Nat. Commun.* **13**, 3327 (2022).

[2] Á. Martín Pendás, E. Francisco, «Decoding real space bonding descriptors in valence bond language», *Phys. Chem. Chem. Phys.* **20**, 12368 (2018).

[3] M. Fugel *et al.*, «Covalency and Ionicity Do Not Oppose Each Other — Relationship Between Si–O Bond Character and Basicity of Siloxanes», *Chem. Eur. J.* **57**, 15275 (2018).

[4] G.B. Bacskay, S. Nordholm, «Covalent Bonding: The Fundamental Role of the Kinetic Energy», *J. Phys. Chem. A* **117**, 7946 (2013).

[5] Z. Chen, C. Zhou, W. Wu, «Seniority Number in Valence Bond Theory», *J. Chem. Theory Comput.* **11**, 4102 (2015).

[6] D.S. Levine, M. Head-Gordon, «Clarifying the quantum mechanical origin of the covalent chemical bond», *Nat. Commun.* **11**, 4893 (2020).

[7] M. Hendzel, M. Fidrysiak, J. Spałek, «Many-particle covalency, ionicity, and atomicity revisited for a few simple example molecules», *J. Phys. B: At. Mol. Opt. Phys.* **55**, 185101 (2022).

[8] M. Hendzel, M. Fidrysiak, J. Spałek, «Toward Complementary Characterization of the Chemical Bond», *J. Phys. Chem. Lett.* **13**, 10261 (2022).

[9] J. Spałek, M. Hendzel, «Exact entanglement correlation complements the chemical bond description», arXiv:2406.06171 [cond-mat.str-el].

[10] B. Robertson, «Introduction to Field Operators in Quantum Mechanics», *Am. J. Phys.* **41**, 678 (1973).

[11] J. Spałek, «Mott Physics in Correlated Nanosystems: Localization–Delocalization Transition by the Exact Diagonalization Ab Initio Method», in: E. Pavariniand, E. Koch (Eds.) «Topology, Entanglement, and Strong Correlations Vol. 10», *Forschungszentrum Jülich*, 2020.

[12] E. Brocławik, M. Fidrysiak, M. Hendzel, J. Spałek, «Interparticle correlations and chemical bonding from physical side: Covalency *versus* atomicity and ionicity», *Adv. Quantum Chem.* **78**, 351 (2023).

[13] J. Spałek, E.M. Görlich, A. Rycerz, R. Zahorbeński, «The combined exact diagonalization — *ab initio* approach and its application to correlated electronic states and Mott–Hubbard localization in nanoscopic systems», *J. Phys.: Condens. Matter* **19**, 255212 (2007).

[14] K. Ruedenberg, «The Physical Nature of the Chemical Bond», *Rev. Mod. Phys.* **34**, 326 (1962).

[15] V.I. Anisimov *et al.*, «First-principles definition of ionicity and covalency in molecules and solids», *J. Chem. Phys.* **160**, 144113 (2024).